Inorganic Chemistry

ARTICLE

pubs.acs.org/IC

Oxidovanadium(IV) Schiff Base Complex Derived from Vitamin B_6: Synthesis, Characterization, and Insulin Enhancing Properties

Tirtha Mukherjee,[†] João Costa Pessoa,[‡] Amit Kumar,[‡] and Asit R. Sarkar*[,†]

[†]Department of Chemistry, University of Kalyani, Kalyani-741235, West Bengal, India

[‡]Centro de Química Estrutural, Instituto Superior Técnico, Technical University of Lisbon, Av. Rovisco Pais 1049-001 Lisboa, Portugal

Supporting Information

ABSTRACT: A new Schiff base, $[H_4pydmedpt]^{2+}\cdot 2Cl^-$, derived from one of the forms of vitamin B_6 has been synthesized by condensation of pyridoxal hydrochloride with *N*,*N*-bis[3-aminopropyl]-methylamine (medpt) and characterized by analytical and spectroscopic methods. The molecular structure is calculated by density functional theory (DFT) procedures, and the donor properties of each individual donor atom are evaluated by calculation of the Fukui function. One pot reaction of pyridoxal and medpt with vanadyl acetylacetonate yields the brown complex $[V^{IV}O(H_2pydmedpt)]^{2+}\cdot 2Cl^-$ **1**, which upon recrystallization from water crystallizes as $[V^{IV}O(pydmedpt)]\cdot 5H_2O$ **2**. The compounds are characterized by analytical and spectroscopic methods, **2** being also characterized by single crystal X-ray diffraction. It displays a slightly distorted octahedral geometry around the vanadium atom involving the coordination of N_{amine}, two N_{imine}, and $O_{phenolato}$ donors of the ligand. One of the phenolato oxygen donors is positioned trans to the terminal O-oxido atom with relatively short $V-O_{phenolate}$ {2.041(3) Å} and long $V-O_{oxido}$ {1.625(4) Å} bond distances when compared to other known compounds. The two different pK_a values (6.0 and 7.9) obtained for **1** are due to protonation of the pyridine ring nitrogen atoms having different basic characters, this being also substantiated by theoretical calculation of the proton affinity of the O- and N- atoms of the molecule. The spin Hamiltonian parameters are obtained from the electron paramagnetic resonance (EPR) spectra, but the A_z value (ca. 155 × 10^{-4} cm^{-1}) is lower than expected by applying the additivity rule for the present set of equatorial donor atoms (ca. 162−163 × 10^{-4} cm^{-1}), this being attributed to the strong trans $V-O_{phenolate}$ bond. The UV−vis transitions and EPR spectral parameters are calculated by DFT procedures, and both the calculated electronic transitions and the hyperfine coupling constants agree well with those experimentally observed. The inhibitory effect of **1** on FFA release and % glucose uptake determined with isolated rat adipocyte cells gave IC_{50} and EC_{50} values lower than for $V^{IV}OSO_4$ and of the same order of magnitude of other reported insulin enhancing vanadium compounds.

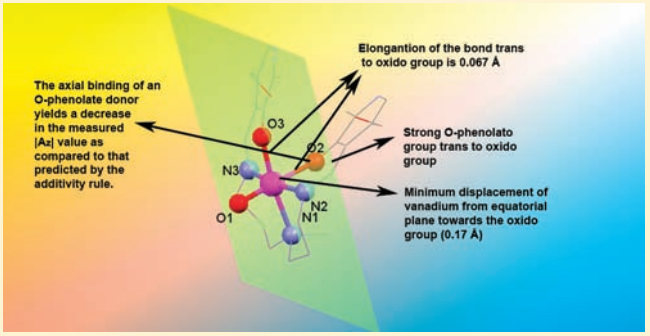

INTRODUCTION

Vanadium plays a number of important roles in biological systems,[1] and in humans its complexes have shown promising activity for the treatment of type II diabetes.[2] Vanadium containing compounds can be used as orally available drugs suitable to ameliorate most of the symptoms of diabetes: high blood sugar, elevated lipid levels, and increasingly damaging secondary complications, including heart disease, cataracts, kidney disease, and peripheral neuropathy.[3] Some chelated vanadium complexes demonstrated superior activity over inorganic vanadium sources through both in vivo and/or in vitro assays of biological effectiveness.[1,4] The first phase I[5] and phase IIa[6] clinical trials of a designed vanadium complex were completed recently. Although insulin mimetic effects of vanadium are well established, there are still differences of opinion among researchers regarding the mechanism of action leading to these effects. Possible modes of action for insulin enhancing activity of vanadium compounds are involved in multiple intracellular action, termed as "ensemble mechanism".[7] The targets for vanadium in this mechanism include protein tyrosine phosphatase (PTPase), phosphatidyl inositol-3-kinase (PI3−K), glucose transporter (GLUT), protein kinase B (PKB), and cyclic nucleotide phosphodiesterase (PDE).[8] In addition to antidiabetic properties, many vanadium complexes are reported to exhibit anticancer properties.[9] Vanadium complexes are also known for their antimicrobial[10] and spermicidal[11] activities.

Pyridoxal acts as a cofactor in enzymatically catalyzed transamination[12] as well as in many other biosynthetic processes such as decarboxylation, racemization of amino acids, and dehydration of serine and threonine.[13] It is also known for its role in anticancer activity.[14] Pyridoxal isonicotinoyl hydrazone class of iron chelators show promising activity as antiproliferative agents.[15] Most of the

Received: December 3, 2010
Published: April 15, 2011

Table 1. Crystallographic Data and Refinement Details for 2

empirical formula	$C_{23}H_{41}N_5O_{10}V$	β (deg)	78.122(5)
fw (g mol^{-1})	598.55	γ (deg)	65.821(5)
space group	$P\bar{1}$	cell volume (Å^3)	1409.7(11)
Z	2	refl. collected	9276
temperature (K)	100	unique refl./$I > 2\sigma(I)$	6669/4815
$d_{(calc)}$ [g cm^{-3}]	1.410	no. of params/restr.	352/0
a (Å)	10.720(5)	radiation	MoKα 0.71069 (nm)
b (Å)	11.925(5)	R[a]/goodness of fit on F^2	0.0777/1.128
c (Å)	12.354(5)	wR_2[b] ($I > 2\sigma(I)$)	0.2881
α (deg)	84.378(5)	resd. dens. [e/Å^3]	+0.948/−1.602

[a] $R = \Sigma||F_o| - |F_c||/\Sigma|F_o|$. [b] $wR_2 = [\Sigma w(F_o^2 - F_c^2)^2/\Sigma w(F_o^2)^2]^{1/2}$.

enzymatic reactions of pyridoxal have been reproduced by non-enzymatic model reactions with pyridoxal and a suitable metal salt acting as a catalyst via the formation of intermediate Schiff base metal complex.[16] Hence, metal complexes derived from pyridoxal Schiff bases have been important for total understanding of the mechanism of action of pyridoxal in vivo, and also for developing bioactive compounds for therapeutic use such as anticancer agents. Since vanadium complexes have anticancer activity of their own, a compound of vanadium with a pyridoxal Schiff base is particularly interesting in this regard. Several metal complexes of Schiff bases derived from pyridoxal and amino acids have been reported.[17] However, studies on metal complexes of Schiff bases derived from pyridoxal and polyamines have been limited by the paucity of authentic complexes, only a few examples being known.[18]

On the other hand medpt is a N-methylated derivative of a naturally occurring polyamine, norspermidine, which is found in some species of plants, bacteria, and algae.[19] It exhibits significant antitumor activity against L1210 leukemia, 3LL carcinoma, and EL4 lymphoma in mice.[20]

Vanadium complexes with N, O donor atoms are known to exhibit insulin enhancing properties.[21] The vanadium picolinato[22a,b] and dipicolinato[22c] complexes are known examples. Therefore, it is relevant to investigate other vanadium complexes with pyridine derivatives possessing N, O donors. Thus, the use of pyridoxal, a pyridine derivative, as one of the building blocks of the ligand design may be advantageous. In fact, it is not expected to yield toxic metabolites, and additionally it may improve solubility of the final complex. Hence, we decided to undertake the synthesis and characterization of a new Schiff base containing the N_3O_2 binding set, H_4pydmedpt$^{2+}\cdot 2Cl^-$, derived from the condensation of pyridoxal and medpt, and of its oxidovanadium(IV) complex. The pentadentate ligand was designed so that a strong phenolato oxygen donor atom may take a position trans to the oxido group, which itself is a rare arrangement of donors for oxidovanadium complexes. The molecular structure, acid−base and spectroscopic properties of the complex, as well as its insulin enhancing activity, are described. Theoretical calculations carried out for the ligand and the complex support the measured spectroscopic properties. Besides its insulin enhancing effect, which is similar to that of other reported oxidovanadium(IV) compounds, the complex is also relevant because of a few unusual structural characteristics.

EXPERIMENTAL SECTION

General Procedures. *Materials.* *N,N*-bis[3-aminopropyl]methylamine (medpt), vanadyl aceylacetonate {$V^{IV}O(acac)_2$}, and pyridoxal hydrochloride were purchased from Aldrich, Milwaukee, U.S.A.. All the other chemicals used were of analytical grade, obtained from local suppliers. Compound medpt was distilled in the presence of activated charcoal prior to use, solvents were dried by standard procedures, and other chemicals were used as received.

Characterization Procedures. Elemental analyses were obtained with a Perkin-Elmer 2400 CHN/O Analyzer. Chloride was determined colorimetrically by the mercuric chloroanilate method, and vanadium was determined colorimetrically by hydrogen peroxide.[23] IR spectra were recorded as KBr pellets on a Perkin-Elmer FT-IR spectrometer (Model: L 120-000A). The electronic spectra were recorded in methanol on a Shimadzu UV-2401 PC spectrophotometer, and the ^{1}H NMR spectra were obtained on a Bruker DPX 300 MHz spectrometer with the common parameter settings. The electron paramagnetic resonance (EPR) spectra were recorded with a Bruker ESP 300E X-band spectrometer at 77 K in methanol and dimethylsulfoxide (DMSO). The spin Hamiltonian parameters were obtained by simulation of the spectra with the computer program of Rockenbauer and Korecz.[24]

For studies of the properties of **1** in aqueous solution, it was dissolved in H_2O (3.00 mM) under argon (initial pH ∼4.5), and EPR and electronic spectra were recorded after stepwise additions of KOH using the above-mentioned instruments. No DMSO or ethylene-glycol was added so that no changes in the composition of the solution occur because of these solvents.

Cyclovoltammetric (CV) measurements were carried out with a potentiostat-galvanostat M 273 (EG&G Princeton Applied Research, U.S.A.) driven by M 270 software. A three-electrode cell was used, consisting of a Pt working disk electrode (0.12 cm), Pt counter, and saturated calomel reference electrode (SCE). CV measurements were performed under nitrogen atmosphere at 27 ± 1 °C in 1.00 mM aqueous unbuffered solution of **1** containing KCl (0.10 M) as supporting electrolyte with a scan rate of 100 mV/s. The pH of the solution was 5.0. The solution was purged with N_2 gas for 5 min before the experiments.

Conductance was measured in 1.00 mM aqueous solution using a Systronic conductivity meter, type 304. The acid dissociation constants of the complex (pK_a values) were estimated by pH-potentiometric titrations of 0.10 mM aqueous solution of the complex with 1 mM carbonate-free standard NaOH solution. Measurements were carried out at 25 ± 0.1 °C, at a constant ionic strength of 0.10 M KNO_3, with a Mettler Toledo DL-28 autotitrater. The reproducibility of the titration points was within 0.005 pH units in the observed pH range: 5.0−9.0.

Single Crystal XRD. Single crystal X-ray diffraction data were collected at 100 K with a Bruker SMART APEX CCD diffractometer using graphite monochromatized Mo−Kα radiation by $\varphi-\omega$ scans. Data reduction and cell refinement were performed by SAINT.[25] Empirical absorption corrections were applied using SADABS.[26] The structure was solved by direct method using SIR-92[27] program and refined by full-matrix least-squares on F^2 using SHELXL-97.[28] Publication material for the complex was prepared by WinGX publication routines.[29] The

dx.doi.org/10.1021/ic102412s |*Inorg. Chem.* 2011, 50, 4349–4361

Scheme 1. Synthesis of the Schiff Base Ligand $[H_4pydmedpt]^{2+}\cdot 2Cl^-$

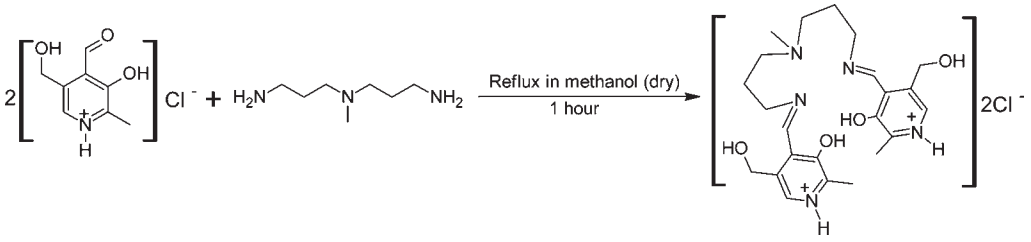

H atoms were all located in a difference map, but those attached to carbon atoms were repositioned geometrically. All the non hydrogen atoms were refined anisotropically. The crystallographic data and refinement details are given in Table 1.

Theoretical Calculations. Theoretical calculations regarding structure optimization, Fukui function (f_k^-) of the ligand and the gas phase proton affinities, UV−vis transitions, EPR spectral parameters of the complex were carried out with the Gaussian 03 software.[30]

The structure of the deprotonated ligand ($pydmedpt^{2-}$) was optimized at the B3LYP[31] level of theory using a 6-31G(d)[32] basis set under the spin restricted closed cell condition. Vibrational frequency calculations were performed on the optimized structure under the same level of theory; these calculations do not give any negative frequencies, confirmimg that the optimized structure represents a true local minimum in the potential energy surface[33]; hence, the optimized structure should be the lowest energy conformer. The functions f_k^- were estimated from single point calculations using the B3LYP[31] method and 6-31G(d)[32] basis set in spin restricted closed cell condition at the optimized geometry, performed for N and $(N-1)$ electron systems, where N is the total number of electrons in the system. In a finite difference approximation, f_k^- of an atom k, in a molecule with N electrons, is expressed by the equation $f_k^- = [q_k(N) - q_k(N-1)]$, where q_k is the electronic population of atom k.[34] The q_k values were calculated by Mulliken population analysis (MPA).

The gas phase proton affinity (PA_g), which is defined as the enthalpy change during the protonation process in the gas phase, was calculated at all possible sites of protonation in the complex. The PA_g values were determined by density functional theory (DFT) using Barone's modified Perdew−Wang 1991 exchange functional[35] and Perdew and Wang's 1991 gradient-corrected correlation functional[36] with a 6-31G(d)[32] basis set.

The EPR parameters of the complex were theoretically calculated using coordinates from its single crystal X-ray structure. Calculations were performed using BHandHLYP (Becke 50−50 method with LYP[37] correlation added) DFT hybrid methods with 6-311G and 6-311G(d,p)[38] basis sets.

The absorption bands in the UV−vis spectrum of the complex in methanol were recorded and compared with the absorption bands predicted by time-dependent DFT (TD-DFT) calculation using the B3LYP method[31] and 6-31G(d)[32] basis set. The single crystal X-ray diffraction data is used for DFT calculations. The contributions of atomic orbitals to the molecular orbitals were calculated by the Chemissian software.[39]

Insulin Enhancing Activity. The insulin enhancing property of the complex was evaluated by both glucose uptake and inhibition of free fatty acids (FFA) release assay in isolated rat adipocytes following the protocol of Adachi and Sakurai.[40] Male Wistar rats (7−8 weeks old) weighing 80−160 g were obtained from local suppliers. Epididymal fat pads were excised from male Wistar rats, anesthetized with ether, cut into the appropriate pieces, and incubated in type IV *collagenase* in Krebs Ringer Bicarbonate (KRB) buffer having pH 7.4, (120 mM NaCl, 1.27 mM $CaCl_2$, 1.20 mM $MgSO_4$, 4.75 mM KCl, 1.20 mM KH_2PO_4 and 24 mM $NaHCO_3$) containing 2% BSA at 37 °C with gentle shaking for one and half hour. The prepared cells were filtered through sterilized cotton gauze and washed with KRB buffer. The cells count was 1.5−2.5 $\times 10^6$ cells/mL, recorded in a hemacytometer after trypan blue staining. Isolated rat adipocyte cells were first incubated at 37 °C for 30 min with various concentrations (0.05 to 1.00 mM) of the complex, or $V^{IV}OSO_4$, in KRB buffer containing 5.0 mM glucose. Adrenaline, 10 μM, was then added to the cell solution, and the resulting solutions were incubated at 37 °C for 3 h. The reactions were frozen by soaking in ice water. Cells were separated with a centrifuge at 3000 rpm for 10 min at 4 °C. Glucose concentrations were measured spectrophotometrically after treatment with trichloroacetic acid and *m*-toluidine. FFA levels were estimated spectrophotometrically by the method described by Itaya and Ui.[41]

Preparations. *Preparation of $[H_4pydmedpt]^{2+}\cdot 2Cl^-$.* The ligand was obtained by refluxing a solution of 0.50 mmol (0.10 g) pyridoxal hydrochloride in 5 mL of dry methanol containing 0.25 mmol (0.04 mL) of medpt for 1 h (Scheme 1). The solvent was evaporated in vacuum, and the residue was purified by elution through a neutral alumina column. The Schiff base fraction was collected as a dark red colored viscous liquid. Yield = 0.05 g (42%). Anal. Calcd. for $C_{23}H_{35}Cl_2N_5O_4$: C, 53.49; H, 6.83; N, 13.56; Cl, 13.73; Found: C, 53.81; H, 6.77; N, 13.42; Cl, 13.66; %. Selected IR peaks with tentative assignments (ν_{max}/cm^{-1}): 3392 (O−H), 2957 (C−H), 1627 (C═N Schiff base coupled to the aromatic ring), 1417 (C−N tertiary amine), 1018 (C−O phenol). UV−vis absorptions: λ_{max}(MeOH)/nm ($\varepsilon/dm^3\ mol^{-1}\ cm^{-1}$) 221 (21200), 251 (10500), 287sh (4400), 339 (4500), 425sh (1200). ^{1}H NMR (DMSO-d_6, δ/ppm): 1.4−2.4 (19H, m, CH_2, Me), 4.6 (4H, s, $CH_{2\ attched\ to\ OH}$), 5.2 (2H, s, $OH_{aliphatic}$), 7.5 (2H, s, CH=N), 8.5 (2H, s, Ph), 10.0 (2H, s, OH_{phenol}).

*Preparation of **1** and **2**.* Compound **1** was synthesized by refluxing a mixture containing 0.50 mmol (0.10 g) of pyridoxal hydrochloride, 0.25 mmol (0.04 mL) of *N*,*N*-bis[3-aminopropyl]methylamine and 0.25 mmol (0.07 g) of $V^{IV}O(acac)_2$ in dry methanol for 3 h (Scheme 2). A brown solid was isolated after addition of acetonitrile, which was collected and recrystallized from a methanol acetonitrile mixture (1:2). The purity of the isolated complex was checked by thin layer chromatography (TLC). Yield = 0.05 g (37%). Important mass spectral peaks: m/z 509.2 (100%) $\{[M+H]^+\}$, 255 (18%) $\{[M+2H]^{+2}\}$. Selected IR peaks with possible assignments (ν_{max}/cm^{-1}): 3356 (O−H), 1621 (C═N Schiff base coupled to the aromatic ring), 1418 (C−N tertiary amine), 1028 (C−O phenol), 907 (V═O), 448 (V−O phenoxo), 379 (V−N). Anal. Calcd. for $C_{23}H_{33}Cl_2N_5O_5V$ (Compound **1**): C, 47.51; H, 5.72; N, 12.05; Cl, 12.20; V, 8.76% Found: C, 47.42; H, 5.63; N, 12.01; Cl, 12.34; V, 8.83%.

Single crystals of $[V^{IV}O(pydmedpt)]\cdot 5H_2O$ **2**, suitable for X-ray diffraction, were obtained by slow evaporation of solvent from a solution of **1** in water having a pH = 5.0. Yield = 15%.

RESULTS AND DISCUSSION

Structure of $pydmedpt^{2-}$. The ligand coordinates to vanadium after deprotonation of two phenolic hydrogen atoms. The structure of the ligand $(pydmedpt)^{2-}$ obtained by DFT procedures (gas phase) is given in Figure 1.

dx.doi.org/10.1021/ic102412s |*Inorg. Chem.* 2011, 50, 4349–4361

Scheme 2. Synthesis of Complex 1

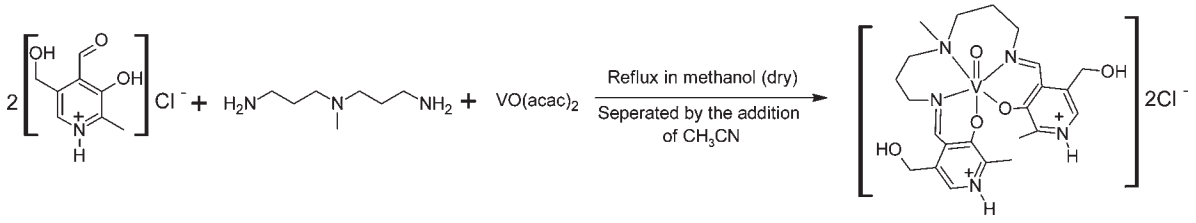

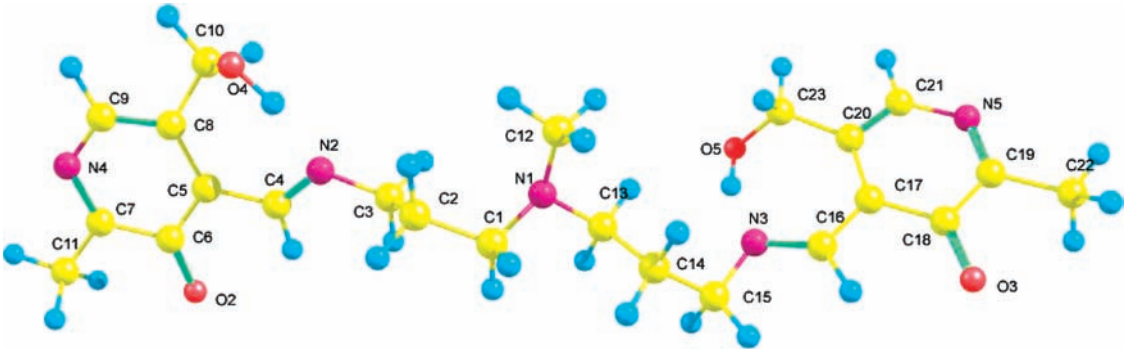

Figure 1. Gas phase molecular structure of pydmedpt^{2-} calculated by DFT (numbering of hydrogen atoms were omitted).

Table 2. Selected Bond Length (Å), Bond Angles (deg), and Dihedral Angles (deg) for pydmedpt^{2-}

	Bond Lengths		
N1−C12	1.455	N1−C1	1.463
N1−C13	1.468	N2−C4	1.296
N3−C16	1.297	O2−C6	1.262
O3−C18	1.262	C5−C6	1.458
C17−C18	1.458		
	Bond Angles		
C1−N1−C13	113.7	N1−C1−C2	114.7
C3−N2−C4	117.7	C15−N3−C16	117.9
C5−C4−N2	127.6	N3−C16−C17	127.4
C12−N1−C13	113.2	C12−N1−C1	113.3
	Dihedral Angles		
C14−C15−N3-C16	126.5	C2−C3−N2-C4	−118.6

Selected bond lengths, bond angles and dihedral angles, dihedral angles for (pydmedpt)$^{2-}$ are given Table 2. The numbering scheme for the ligand is presented in Figure 1.

The two imine groups are in trans orientation in the optimized gas phase structure of pydmedpt^{2-} (Figure 1). The structures of the isomers with one or both imine groups in cis orientation were also optimized, under the same level of theory. The all trans isomer of the ligand is more stable than its cis-trans or all cis isomer; the differences in energy between the optimized isomeric forms are 24.3 and 37.6 kcal mol^{-1}, respectively. The imine nitrogen and the phenolic oxygen atoms in this optimized trans form are obviously not sterically oriented for chelation toward the central vanadium atom. Hence, for complex formation, the ligand in its deprotonated form is forced to undergo a structural rearrangement to bind vanadium. The dihedral angles between the pair of planes C2, C3, N2 and C4, N2, C3 and also the other pair of planes between C16, N3, C15 and N3, C15, C14 in the ligand undergo an angular flip in the complex. A similar structure was obtained when optimization was performed in aqueous solution; the structural parameters are given in Supporting Information, Table S3.

Calculation of the Fukui Function. The condensed Fukui function values f_k^- may be used to identify the most suitable atoms for electrophilic attack,[42] and they were determined to investigate the ligation properties of the donor atoms of the deprotonated ligand pydmedpt^{2-}. Selected f_k^- values are given in Table 3. The atom numbering scheme is the one used in Figure 1.

According to the values of the Fukui functions presented in Table 3, the $O_{phenolate}$ donor atoms (O2, O3) may be anticipated to be much stronger donor atoms than the aliphatic $O_{alcohol}$ atoms (O4, O5). The aliphatic $O_{alcohol}$ atoms are adequately placed for chelation in the ligand, but the phenolate oxygens coordinate to vanadium in the actual complex. According to Table 3 the $N_{pyridine}$ donors (N4, N5) are among the strongest donor sites. However, they are not coordinated in the complex since there are no suitable donor atoms in the ortho position to give the possibility of a chelation effect. The tertiary nitrogen atom, N_{amine} (N1), which has a negative value of f_k^-, may be expected to be a very weak donor, yet its position in the ligand forces it to coordinate to vanadium. In this particular situation there is nothing which could significantly increase the relative donor property of the tertiary nitrogen in the complex. Therefore, the tertiary nitrogen is expected to continue as the weakest donor, and thus the corresponding bond length to vanadium is expected to be longer than those of the imine nitrogens. This expectation is indeed confirmed by the molecular structure determined by X-ray diffraction as the bond length between vanadium and the tertiary nitrogen [2.224(4) Å] is significantly longer than the distance between vanadium and the two N_{imine} donors [2.086(4), 2.094(4) Å], thereby indicating a weak bond.

dx.doi.org/10.1021/ic102412s |*Inorg. Chem.* 2011, 50, 4349–4361

Table 3. Selected f_k^- Values Calculated for pydmedpt^{2-}

atom	O2 ($O_{phenolate}$)	O3 ($O_{phenolate}$)	O4 ($O_{alcohol}$)	O5 ($O_{alcohol}$)	N1 (N_{amine})	N2 (N_{imine})	N3 (N_{imine})	N4 ($N_{pyridine}$)	N5 ($N_{pyridine}$)
f_k^-	0.0345	0.0395	0.0138	0.0149	−0.0026	0.0285	0.0285	0.0385	0.0447

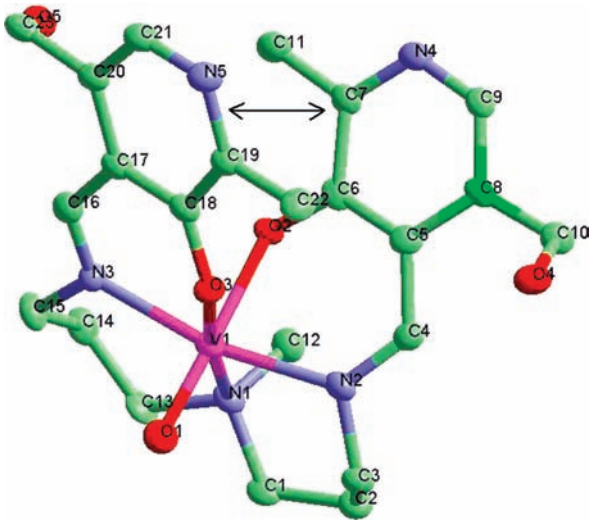

Figure 2. Molecular structure and atom numbering scheme of **2**, as 50% thermal ellipsoids. The $\pi-\pi$ stacking interactions between the aromatic rings are shown by a double headed arrow. The hydrogen atoms are omitted for clarity.

Crystal Structure. Complex **2** was crystallized from the aqueous solution of complex **1** upon slow evaporation of the solvent. The compound changes its protonation state upon formation of the crystal, and the Cl^- anions initially present in the solid isolated are not present in **2**. The complex crystallizes as $[V^{IV}O(pydmedpt)]\cdot 5H_2O$, with five water molecules per asymmetric unit. The structure of the complex is shown in Figure 2, and selected bond lengths and angles are given in Table 4.

The compound $[V^{IV}O(pydmedpt)]$ (Figure 2) corresponds to a slightly distorted octahedral geometrical arrangement of donor atoms around the vanadium center, involving the O_{oxido} atom, one tertiary amine nitrogen donor (N_{amine}), two N_{imine} and two $O_{phenolate}$ donors. One of the $O_{phenolate}$ donors is bound trans to the O_{oxido}, with a relatively short $V-O_{phenolate}$ bond of 2.041(3) Å, when comparing with those expected for bonds trans to the oxido group.

The distortion from an octahedral geometry because of the terminal oxido group in oxidovanadium complexes may be evaluated by (a) displacement of the vanadium atom from the equatorial plane toward the oxido group (ΔD), and (b) elongation of the bond trans to the oxido group (ΔL).

The displacement of the vanadium atom toward the terminal oxido group, ΔD, from the least-squares plane,[43] defined here by atoms O3, N3, N1, and N2 is only 0.17 Å. The V1−O2 bond trans to the oxido group is elongated by only 0.067 Å as compared to the other $V-O_{phenolato}$ bond (V1−O3). This displacement from the equatorial plane and the elongation of the V−O bond trans to the terminal V═O group are small compared to the usual values found for $V^{IV}O$-complexes in the literature[44] (Table 5).

The relatively small difference between the V1−O2 and V1−O3 bond distances, that is, to the trans and cis phenolato oxygen atoms, and also the small value of ΔD makes $[V^{IV}O(pydmedpt)]$ closer to an octhedral geometry than most other similar oxidovanadium complexes (Table 5). The amount of elongation ΔL and other relevant data for $[V^{IV}O(pydmedpt)]$ and a few selected complexes from the literature are given in Table 5.

Table 4. Selected Bond Lengths (Å) and Bond Angles (deg) for 2

bond lengths (Å)		bond angles (deg)	
V1−O1	1.625(4)	O1−V1−O2	175.6(16)
V1−O2	2.041(3)	O1−V1−N1	88.1(17)
V1−O3	1.974(4)	O1−V1−N3	93.9(17)
V1−N1	2.224(4)	O2−V1−N1	88.3(14)
V1−N2	2.086(4)	O2−V1−N2	83.6(15)
V1−N3	2.094(4)	O3−V1−N3	87.3(15)

This tendency toward an octahedral geometry in **2** is most likely caused by the mutual cancellation of the strong trans effect of the oxido group and that of the $O_{phenolato}$ donor, this resulting in a weaker than normal V═O bond. Accordingly, the V═O bond length [1.625(4) Å] is on the higher side compared to reported literature values,[44] and the V═O stretching frequency is low (907 cm^{-1}), reflecting the relatively weak nature of the present V═O bond.

Octahedral oxidovanadium complexes in the presence of both N- and O- donors often prefer the N- donor in trans position with respect to O_{oxido}.[44] If the bond trans to O_{oxido} is strong, namely, the present $O_{phenolato}$-V bond, it will tend to weaken both bonds by trans effect from each other. As described, in $[V^{IV}O(pydmedpt)]$ a quite strong $O_{phenolato}$-V bond is established trans to O_{oxido}, and to our knowledge only one similar example, $V^{IV}O(SALIMH)_2\cdot 3C_2H_5OH$ (Table 5), was reported.[45] In this compound the effect of mutual weakening also exists but is less pronounced (Table 5). The reason for this unusual disposition of donor atoms around the vanadium center in **2** is partly because this arrangement facilitates the proximity of the two pyridine rings. Thus, the destabilizing trans effect is compensated by the establishment of $\pi-\pi$ stacking interactions between the two pyridine rings. In fact, the two pyridine rings are close to each other, oriented at 30.78° and at a distance of 4.263 Å between their centroids, indicating the existence of $\pi-\pi$ stacking interactions (Figure 2). This is also supported by the results of the theoretical calculations, where considerable electron density was found in occupied molecular orbitals (MOs) in between carbon atoms C18, C19 of one of the pyridine rings, and carbon atoms C6, C7 of the other ring (atom numbering scheme follows as in Figure 2). A representation of these MOs is presented in Figure 3.

The crystal is held by an intricate network of hydrogen bonds involving five molecules of lattice water. The details of bond distances and angles of hydrogen bonds and their diagrammatic representations are given in Supporting Information, Table S1, Figures S2, S3, and S4. Two primary alcohol atoms (O5, O4), two pyridine nitrogen atoms (N5, N4), the O_{oxido} (O1), and one

dx.doi.org/10.1021/ic102412s |Inorg. Chem. 2011, 50, 4349–4361

Table 5. Comparison of Distortion from Octahedral Geometry Due to the Terminal Oxido Group in Several 6-Coordinated $V^{IV/V}$ O-Complexes

complex	ΔD (Å)	ΔL (Å)	V=O (Å)	reference
$V^{IV}O(pydmedpt)]\cdot 5H_2O$	0.170	0.067	1.625(4)	present work
$V^{IV}O(SALIMH)_2\cdot 3C_2H_5OH$[a]	0.220	0.118	1.610 (4)	45
$[V^{IV}O(H_2O)(5MeOpic)_2]\cdot 3.5H_2O$[b]	0.295	0.133	1.597(3)	46
$V^{IV}O(SalimRH)(acac)$[c]		0.195	1.603(3)	47
$[V^{IV}O(dipic)(HMDCI)]^{-}$[d]		0.280; 0.269	1.599(1)	47
$[V^{IV}O(DMSO)_5]I_2$[e]		0.154	1.603	48
$V^{V}O(psal)(L_2)\cdot H_2O$[f]	0.280	0.273	1.576(3)	49

[a] HSALIMH = 4-(2-(salicylideneamino)ethyl)imidazole. [b] 5MeOpic =5-acetylpicolinic acid. [c] SalimRH = *N*-(*o*-hydroxyphenyl) histamine. [d] H_2MDCI = 1-methyl-4,5-dicarboxyimidazole, dipic =2,6-pyridinedicarboxylic acid. [e] DMSO = dimethyl sulphoxide. [f] psal = salicylaldimine of 2-picolylamine.

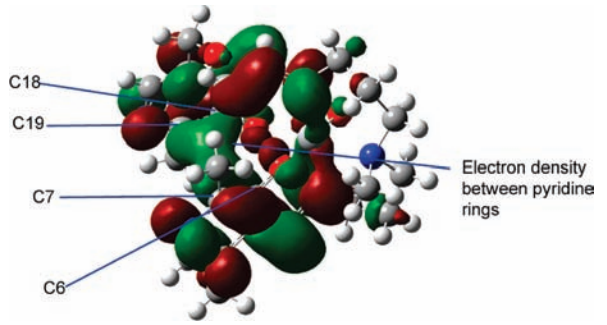

Figure 3. Singly occupied molecular orbital (SOMO) of the molecular structure calculated by the B3LYP method[31] using a 6-31G(d)[32] basis set.

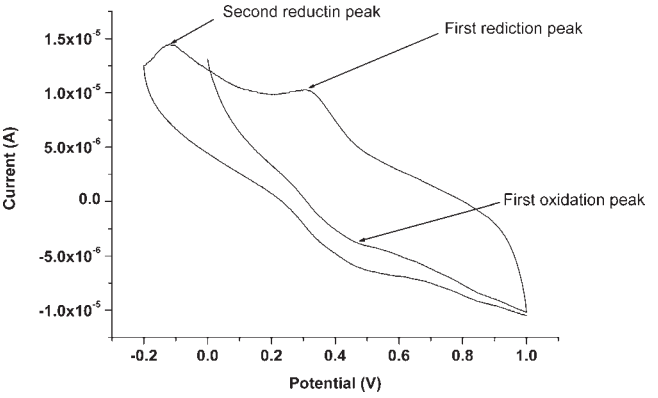

Figure 4. Cyclic voltammogram of **1**.

$O_{phenolate}$ (O3) are involved in hydrogen bonding along with the five water molecules. Interestingly, the second $O_{phenolate}$ (O2) does not take part in hydrogen bonding. The five water molecules are hydrogen bonded to each other forming a zigzag chain. Among the five water molecules, OW3 is involved in H bonds to four H atoms, while the rest are involved with three H atoms. Each of these water chains are hydrogen bonded to six different complex molecules. Again, each complex molecule is hydrogen bonded to six such water chains.

Complex **2** was optimized in the gas phase and also in aqueous solution by DFT methods; their structural parameters are almost identical to those obtained by the X-ray diffraction method. The details are given in the Supporting Information, Table S4.

Electrochemical Studies. The ligand solution is electrochemically inactive in the working potential region so all electrochemical changes observed are due to the vanadium center. The cyclic voltammogram for complex **1** shows a quasi reversible redox couple at peak potential of +0.45 and +0.30 V attributed to the V(IV)/V(V) couple[50] and an irreversible change at −0.15 V (Figure 4) due to the V(IV)/V(III) couple.[51] The irreversibility of the V(IV)/V(III) couple is in accordance with the reports in the literature that reduction of vanadyl complexes to the trivalent state are usually irreversible, because such reduction typically entails loss of the vanadyl oxygen[52] (Scheme 3).

Crans, observing that all compounds showing effectiveness as insulin enhancing agents in vivo underwent irreversible aqueous redox chemistry as determined by cyclic voltammetry, developed the hypothesis that a vanadium compound with reversible redox chemistry would not show effectiveness as an insulin enhancing agent in vivo.[53] According to this hypothesis, our compound has good prospects to show insulin enhancing activity in vivo

Scheme 3. Possible Explanation of the Electrochemical Behavior of $[V^{IV}O(H_2pydmedpt)]^{2+}$, Assuming That the Ligand Retains Its Protonation State in the Oxidation States Considered

$$[V^{V}O(H_2pydmedpt)]^{3+} \rightleftharpoons [V^{IV}O(H_2pydmedpt)]^{2+} \longrightarrow [V^{III}(H_2pydmedpt)]^{+} \longrightarrow \text{Decomposition}$$

Table 6. Calculated Gas Phase Proton Affinities (kcal mol^{-1}) for Several Atoms of $[V^{IV}O(pydmedpt)]$

protonation site	O1	O2	O3	O4	O5	N5	N4
proton affinity value	225.76	224.42	232.50	211.65	209.47	250.97	253.21

Calculation of Protonation Sites of $[V^{IV}O(pydmedpt)]$. The calculated proton affinity values (PA_g) for the different protonation sites are given in Table 6 (atom numbering as in Figure 2). The calculated values are in the range 209.47 to 253.21 kcal mol^{-1} as found in the literature.[54] This analysis shows that the two $N_{pyridine}$ atoms have the higher values of PA_g. Hence, in the complex in its dichloride form both pyridine nitrogen atoms will be protonated. The small difference of the PA_g between the N4 and N5 nitrogens (Table 6) arises because of the distinct relative positions of the pyridine rings with that of the terminal V=O group. Nitrogen N4 of the pyridine ring linked to the $O_{phenolato}$ trans to the V=O bond is more basic than nitrogen N5. Hence, from the proton affinity values, the two pyridine nitrogen atoms

dx.doi.org/10.1021/ic102412s |*Inorg. Chem.* 2011, 50, 4349–4361

Table 7. Molar Conductance and pK_a Values of Aqueous Solutions of 1

Parameter	value
molar conductance (S m^2 mol^{-1})	0.0203
pK_{a1}	6.0
pK_{a2}	7.9

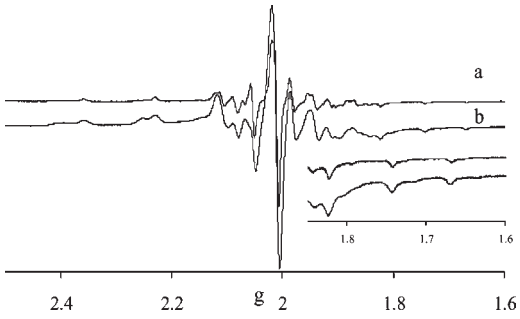

Figure 5. First derivative EPR spectra of frozen solutions of $[V^{IV}O(H_2pydmedpt)]^{2+}\cdot 2Cl^-$ **1**, (4.00 mM) (a) in MeOH; (b) in DMSO. Amplified parts of the high field region of the same spectra are also included to better visualize this part of the spectra.

will have different basicity, as has been evidenced by the finding of two different pK_a values (see below).

Conductance and pK_a of Complex 1. The molar conductance and pK_a values obtained are given in Table 7.

The conductance data indicate the formation of 2:1 electrolyte species in aqueous solution of **1**. This again supports the formulation of complex **1** as $[V^{IV}O(H_2pydmedpt)]^{2+}\cdot 2Cl^-$, which in aqueous solution yields $[V^{IV}O(H_2pydmedpt)]^{2+}$ and two Cl^- anions.

To check if the pK_a values could be due to hydrolysis of $[V^{IV}O(H_2pydmedpt)]^{2+}$ and equatorial binding of OH^-, $[V^{IV}O(H_2pydmedpt)]^{2+}\cdot 2Cl^-$ **1** was dissolved in water and EPR and visible spectra of the solutions were recorded as a function of pH. No indication of equatorial OH^- binding was found up to at least pH = 8.5; therefore the pK_a values of 6.0 and 7.9 should be due to dissociation of the protons bound to the $N_{pyridine}$ atoms of the pyridoxal ring.

The two pK_a values estimated for complex **1** obtained from titration of a solution of **1** with base indicate different environments for the two pyridine nitrogen atoms N4 and N5, resulting in different basic characters. The $O_{phenolato}$ trans to the oxido group has a weaker VO bond, and the global negative charge delocalized over the pyridine ring will be larger. Hence, the nitrogen N4 of pyridine ring (Figure 2) should be more basic, and a pK_a of 7.9 can be assigned to it. This is supported by the calculated PA_g value of N4, which is 2.24 kcal mol^{-1} higher than that of N5 (Table 7).

Kawabe et al. have demonstrated that the insulin enhancing activity of some isomers of vanadyl amino acid complexes increase with decreasing pK_a of the amino acid.[55] The first pK_a value of the complex is below the pK_a value of these amino acid complexes studied.

EPR Spectra. The X-band EPR spectra of the complex **1** in both methanol and DMSO as solvents were recorded and are presented in Figure 5. Figure 6 depicts EPR spectra of Complex **1** (3.00 mM) dissolved in H_2O under argon (initial pH ~ 4.5), and

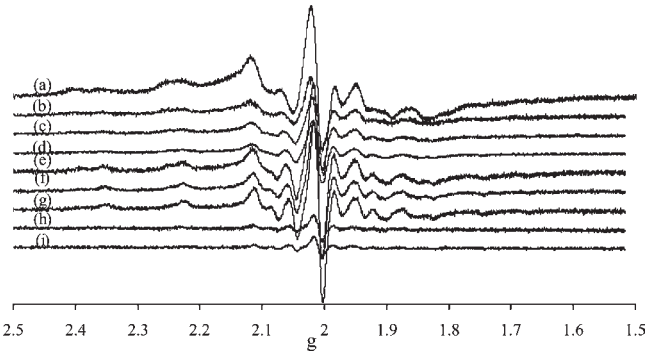

Figure 6. First derivative EPR spectra (at 77 K) of $[V^{IV}O(H_2pydmedpt)]\cdot 2Cl^-$ **1** (3.00 mM) dissolved in H_2O under argon. As no DMSO or ethylene-glycol was added, the EPR spectra shows rather broad features. (a) fresh solution pH ~ 4.47; (b)−(i): upon stepwise additions of KOH; (b) pH ~ 4.61; (c) pH ~ 5.20; (d) pH ~ 5.82; (e) pH ~ 6.57; (f) pH ~ 7.40; (g) pH ~ 8.50; (h) pH ~ 9.40; (i) pH ~ 10.10.

Table 8. Spin Hamiltonian Parameters Obtained from EPR Spectra[a]

solvent	$\lvert A_x, A_y\rvert \times 10^{-4}$ cm^{-1}	g_x, g_y	$\lvert A_z\rvert / \times 10^{-4}$ cm^{-1}	g_z
MeOH	53	1.983	155.2	1.954
	51	1.987	162.9	1.953
	ca. 52	ca. 1.982	ca. 167	ca. 1.950
DMSO	53	1.982	156.4	1.951
	53	1.980	165.2	1.950

[a] Under axial symmetry $A_x = A_y = A_\perp$ and $A_z = A_\parallel$. Note that in the text we used the values of $|A_x|$, $|A_y|$, $|A_z|$, as usual in most texts.

Table 9. Theoretical and Experimental ^{51}V Anisotropic Hyperfine Coupling Constants $|A_z|$, $|A_x|$, or $|A_y|$

parameters $\lvert A_z\rvert$, $\lvert A_x\rvert$, or $\lvert A_y\rvert$	DFT calculation BHandHLYP/6-311G	DFT calculation BHandHLYP/6-311G(d,p)	experimental values
$\lvert A_z\rvert$ ($\times 10^{-4}$ cm^{-1})	148.6	154.5	155.2−156.5
$\lvert A\rvert$ ($\times 10^{-4}$ cm^{-1})	47.9	62.7	
$\lvert A\rvert$ ($\times 10^{-4}$ cm^{-1})	56.4	53.7	51−53

after stepwise additions of KOH; the corresponding spin Hamiltonian parameters are given in the Supporting Information, Table S2. No DMSO or ethylene-glycol was added so that no changes in solution occur because of these solvents.

The observation of the high-field region of the spectra of Figure 5 indicate the presence of at least 3 distinct species in solution when using MeOH, while in DMSO at least two distinct species are detected. The spin Hamiltonian parameters determined by simulation of the experimental EPR spectra are included in Table 8.

The major species, with A_z 155−156.5 $\times 10^{-4}$ cm^{-1}, possibly does not have axial symmetry, but because of the presence of several species, rhombic distortions were not considered in the simulation of spectra. The values of A_z can be estimated using the "additivity relationship" proposed by Wüthrich and Chasteen,[56,57] with estimated accuracy of $\pm 1.5 \times 10^{-4}$ cm^{-1}. Taking the contributions of each equatorial donor atom ($O_{phenolate}$ ~ 38.9,[57]

dx.doi.org/10.1021/ic102412s |Inorg. Chem. 2011, 50, 4349–4361

Scheme 4. Schematic Representation of the Binding Set of Complex 1 and of Other Possible Binding Modes[a]

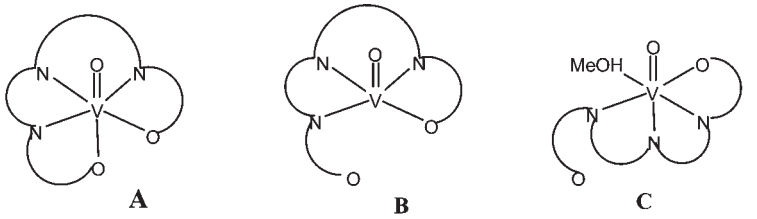

A_z^{est} ~155-156.5×10^{-4} cm^{-1} A_z^{est} ~162-163×10^{-4} cm^{-1} A_z^{est} ~167×10^{-4} cm^{-1}

[a] The corresponding $|A_z|$ values ($\times 10^4$ cm^{-1}) predictexd by the additivity rule[56,57] are also included.

$N_{imine} \sim 41-42$,[1,58,59] $N_{amine} \sim 40.1$,[57] $O_{DMSO} \sim 41.9$,[18] $O_{MeOH} \sim 45.6$[57]), we find that for the expected equatorial donor set of $O_{phenolate}$, N_{amine}, and two N_{imine}, the value of $A_z^{est} = (162-163) \times 10^{-4}$ cm^{-1} is predicted, which does not agree with the experimental value of $(155-156.5) \times 10^{-4}$ cm^{-1}.

Many attempts to correctly predict the EPR parameters for $V^{IV}O$-complexes by theoretical calculations have been carried out in the literature.[60] The combination of the BHandHLYP functional and 6-311g(d,p) basis set was reported to give the best results in these type of calculations.[61] We also carried out theoretical calculations for [$V^{IV}O$(pydmedpt)] by DFT procedures, using (i) BHandHLYP[37]/6-311G[38] and the (ii) BHandHLYP[37]/6-311G(d,p)[38] levels. The calculated $|A_z|$ values (Table 9) are lower than the $|A_z^{est}|$, and those obtained by BHandHLYP/6-311G(d,p) levels are closer to the experimental one. Recently Garribba and co-workers[62] rationalized this type of anomalous behavior found for the A_z of several $V^{IV}O$ complexes, explaining the decrease in the $|A_z|$ as due to the axial binding of solvent molecules in a square pyramidal coordination environment, and having its origin mainly in the $|A_{iso}|$ term (A_{iso}, isotropic contribution from the Fermi contact). Therefore, it is concluded that for [$V^{IV}O$(pydmedpt)] the axial binding of an $O_{phenolate}$ donor in complex **1** yields a decrease of about $7-8 \times 10^{-4}$ cm^{-1} in the measured $|A_z|$ as compared to that predicted by the additivity rule.

In MeOH a second species is detected with $A_z = 162.9 \times 10^{-4}$ cm^{-1}. This agrees with the A_z predicted for the binding set $(O_{phenolate}, N_{amine}, 2 \times N_{imine})_{equatorial}$, and probably corresponds to the complex with no axially bound $O_{phenolate}$ (see Scheme 4, B).

In MeOH a third EPR active species is also detected in small concentration with an A_z of ~167×10^{-4} cm^{-1} which probably corresponds to a partially hydrolyzed complex. In Scheme 4, one possible structure (**C**) is represented, where one of the equatorial donor atoms is substituted by a MeOH ligand. This corresponds to a predicted[56,57] increase in the A_z value of about $4-6 \times 10^{-4}$ cm^{-1} in satisfactory agreement with the increase in the A_z value obtained experimentally.

Since no DMSO or ethylene-glycol was added, the EPR spectra in water show rather broad features; nevertheless, it is clear that the overall pattern/features of the EPR active species remain approximately the same upon adding KOH, no indication of equatorial OH^- binding up to at least pH = 8.5 [spectrum (g)] being noticed, in agreement with the expected deprotonations (pK_a's at ca. 6.0 and 7.9) being due to dissociation of the protons bound to the pyridine nitrogens of the pyridoxal ring. The changes observed in spectra (h) and (i), namely, the lower intensity of the signal, are most probably due to oxidation of the V^{IV}- to V^V-complexes. In almost all these spectra in water two species are detected with A_z of about 154.5 and 170 $\times 10^{-4}$ cm^{-1}, exceptions being (h) and (i), where the low intensity only allows to detect the signal at about 154.5×10^{-4} cm^{-1}. The species with A_z of about 163×10^{-4} cm^{-1} detected in MeOH and DMSO is not detected in aqueous solution. Overall these spectra confirm that the pattern of the EPR signals is preserved in the pH range 4.5−10.0, the nature of the EPR active species present being preserved, the binding modes of these being similar to those observed in methanol.

Table 10. Theoretical and Experimental Electronic UV-visible Transitions for [$V^{IV}O$(pydmedpt)][a]

experimental band/nm (ε/dm^3 mol^{-1} cm^{-1})	TD-DFT peak/nm (osc. str. × 10^5)	contributions
750 (30)	735 (10)	$HOMO_\alpha \rightarrow LUMO_\alpha$
		$HOMO_\alpha \rightarrow (LUMO+3)_\alpha$
547 (60)	536 (40)	$HOMO_\beta \rightarrow LUMO_\beta$
380 (1 300)	381 (440)	$(HOMO-4)_\beta \rightarrow (LUMO+1)_\beta$
350 (1 500)	352 (700)	$(HOMO-2)_\alpha \rightarrow (LUMO+2)_\alpha$
		$(HOMO-2)_\beta \rightarrow (LUMO)_\beta$

[a] In $V^{IV}O$-complexes the bands at about 750 nm are assigned to $d_{xy} \rightarrow d_{xz}$, d_{yz} transitions, and those at about 550 nm to $d_{xy} \rightarrow d_{x^2-y^2}$ transitions. As mentioned in the text, from our calculations, it is not possible to confirm these assignments in the case of [$V^{IV}O$(pydmedpt)].

UV−vis Spectra. The experimental and calculated λ_{max} of bands observed along with their assignments for [$V^{IV}O$(pydmedpt)] are presented in Table 10. The molecular orbitals involved in the transitions, as calculated by DFT procedures, are shown in Figure 7.

The experimental electronic spectra for hexacoordinated $V^{IV}O$-complexes having a N,O coordination environment have been interpreted either on the basis of d-d transitions involving vanadium and/or on the basis of charge transfer bands or $n \rightarrow \pi^*$ or $\pi \rightarrow \pi^*$ transitions from the ligand. Our present theoretical calculations predict that each molecular orbital is formed by the combination of a large number of atomic orbitals. There is no clear dominant contributor to the molecular orbitals involved in the transitions. To make the situation more complicated each spectral band arises because of multiple transitions between the molecular orbitals. Contributions of different atomic orbitals to the molecular orbitals involved in transitions are given in Table 11. From Table 11 it is clear that no atomic orbital has at least 25% contribution to a molecular orbital. Therefore, in this particular case the nature of the spectral bands cannot be expressed in terms of any

dx.doi.org/10.1021/ic102412s |Inorg. Chem. 2011, 50, 4349–4361

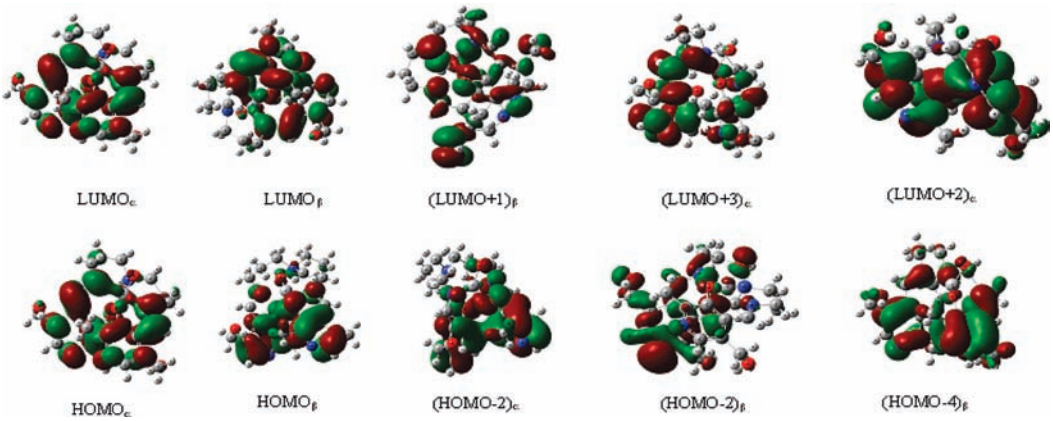

Figure 7. Most important molecular orbitals involved in electronic transitions of complex [$V^{IV}O$(pydmedpt)].

Table 11. Major Contributions of Atomic Orbitals to the Molecular Orbitals Involved in UV-visible Transitons[a]

molecular orbital	% Mulliken contribution of atomic orbitals[b] [contribution (atom type number-atomic orbital)]
HOMO$_\alpha$	08 (O 3-p$_y$), 07 (O 3-p$_z$), 06 (C 21-p$_z$), 06 (C 19-p$_z$), 06 (V 1-d$_{yz}$), 06 (V 1-d$_{xy}$), 05 (C 17-p$_z$)
HOMO$_\beta$	09 (O 3-p$_z$), 07 (C 21-p$_z$), 06 (C 19-p$_z$)
(HOMO-4) $_\beta$	11 (C 20-p$_z$), 09 (C 17-p$_z$), 07 (N 5-p$_z$), 05 (N 3-p$_z$)
(HOMO-2)$_\alpha$	12 (V 1-d$_{xy}$), 09 (V 1-d$_{yz}$)
(HOMO-2)$_\beta$	11 (N 4-p$_x$), 05 (N 5-p$_x$)
LUMO$_\alpha$	08 (C 16-p$_z$), 08 (N 3-p$_z$)
(LUMO+3)$_\alpha$	17 (V 1-d$_{yz}$), 12 (V 1-d$_{xy}$), 08 (O 1-p$_y$), 08 (V 1-d$_{z^2}$)
LUMO$_\beta$	10 (C 4-p$_z$), 07 (N 2-p$_z$)
(LUMO+1)$_\beta$	12 (C 16-p$_z$), 10 (N 3-p$_z$)
(LUMO+2)$_\alpha$	16 (V 1-d$_{x^2-y^2}$), 15 (V 1-d$_{z^2}$), 10 (V 1-d$_{xz}$), 08 (V 1-d$_{yz}$), 07 (O 1-p$_x$)

[a] Only atomic orbitals having 5% or more contributions are listed; contributions are calculated by the Mulliken method. [b] Atom numbering scheme as in Figure 2.

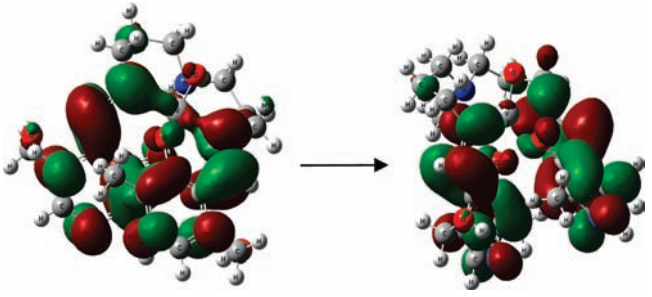

Figure 8. HOMO$_\alpha$→LUMO$_\alpha$ transition in [$V^{IV}O$(pydmedpt)] is shown as a representative case.

specific dominant orbital contributor. The shapes of the molecular orbitals (Figure 8) clearly demonstrate the absence of any major contributor like d or π orbitals. However, from the representation of the orbitals (Figure 7), it is clear that the aliphatic chain and the N_{amine} atom are least involved in the formation of molecular orbitals responsible for electronic transitions. The molecular orbitals

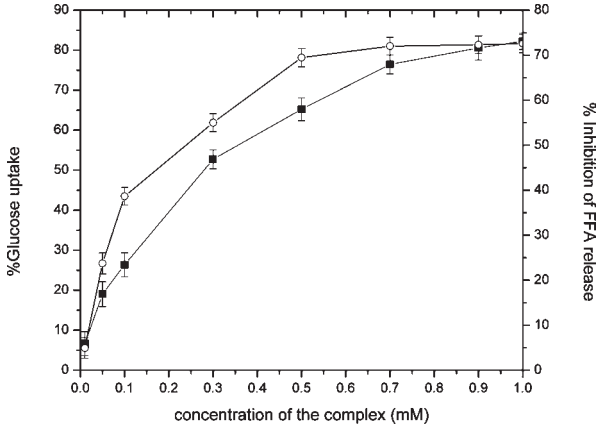

Figure 9. Dependence of % glucose uptake(■) and % inhibition of FFA release (○) on the concentration of **1**.

Table 12. Some Selected IC_{50} and EC_{50} values [a]

compound	IC_{50}	EC_{50}	reference
1	0.27	0.75	present work
$V^{IV}O(pa)_2$[b]	0.73	0.61	40
$V^{IV}O(6mpa)_2$[c]	0.60	0.71	40
VO^{IV}−PYD[d]	0.62		66
VO^{IV}-γ-PGA[e]	0.45	0.90	67
[$V^{IV}O$(L1)(H_2O)][f]	0.69		68
[$V^{IV}O$(Hhpic-O,O)(Hhpic-O,N)(H_2O)]·3H_2O[g]	0.78		69

[a] The values are presented in comparison to values of $V^{IV}OSO_4$, expressed as 1.00 mM. [b] pa = picolinate. [c] 6mpa =6-methylpicolinate. [d] VO-PYD = bis(*N*-methyl,*N*′-D-glucamine-dithiocarbamate)oxidovanadium. [e] VO-γ-PGA = vanadyl-poly(c-glutamic acid). [f] L1 = *N*-(4-Imidazolylmethyl)iminodiacetate. [g] H_2hpic =3-hydroxypyridine-2-carboxylic acid.

involved in UV−vis transitions are mainly located over the two pyridine rings, the imino groups, the phenolato oxygens, and vanadium.

The visible spectra in aqueous solution at different pH show rather broad bands (see Supporting Information, Figure S5), the spectral bands being less resolved than in MeOH, as found with, for example, other V^{IV}-Schiff base systems with

dx.doi.org/10.1021/ic102412s |*Inorg. Chem.* 2011, 50, 4349–4361

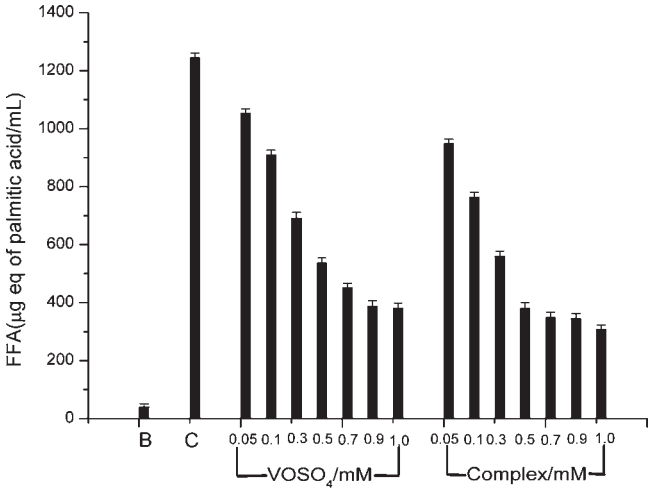

Figure 10. Inhibitory effects on FFA release of solutions of $V^{IV}OSO_4$ and **1** in the concentration range 0.05−1.00 mM. **B** is the blank, and **C** is the control (in presence of epinephrine only).

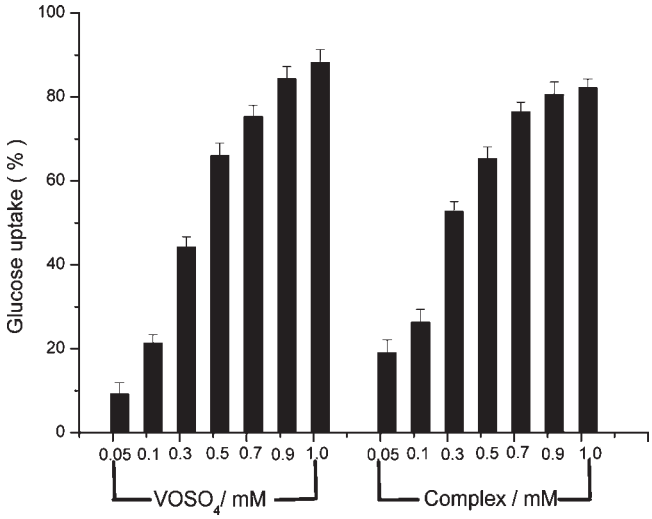

Figure 11. Enhancing effect of solutions of $V^{IV}OSO_4$ and **1** on the glucose uptake ability by cells. The concentration range tested was 0.05−1.00 mM.

N-salicylideneamino acidato ligands.[18d,58] This may be partly due to the formation of a small amount of the EPR-silent $[(V^{IV}O)_2(OH)_5^-]_n$ species,[63] which gives rise to strong ligand to metal charge transfer bands. The pattern of the spectra in the 600−1000 nm range is more or less preserved up to pH ∼ 7.6, but the absorbance decreases significantly for pH > 7.6, probably because of oxidation of V^{IV}- to V^{V}-complexes, as also concluded from the intensity of the corresponding EPR signals.

Insulin Enhancing Properties. The inhibitory action of the complex on the FFA-release from isolated rat adipocytes treated with epinephrine (adrenaline) was evaluated as percentage inhibition with respect to control. The glucose-uptake enhancing ability of the complex was evaluated, based on percentage decrease in the glucose concentrations in the medium with respect to control. Here, control was the concentration of FFA or glucose in the medium, in which cells were incubated containing epinephrine, in the absence of $V^{IV}OSO_4$ or complex **1**.

The dependence of % glucose uptake and % inhibition of FFA release on concentration of the complex is shown in Figure 9.

The EC_{50} value, that is, the concentration of $V^{IV}OSO_4$ or complex at 50% glucose uptake, was found from the plot of log of concentration of vanadium compound against % glucose uptake, and by fitting it with a four parameter log EC_{50} model.[64] The values were found to be 0.39 ± 0.11 mM for **1** and 0.52 ± 0.16 mM for $V^{IV}OSO_4$. The IC_{50} value, that is, the concentration giving 50% inhibition of free fatty acid (FFA) release, was found in a similar way. The values in this case are 0.12 ± 0.06 mM for **1** and 0.44 ± 0.19 mM for $V^{IV}OSO_4$. The EC_{50} and IC_{50} values of some complexes reported in the literature are given in Table 12. The values are presented in comparison to values of $V^{IV}OSO_4$, expressed as 1.00 mM.

The amounts of FFA release against the concentration of solutions containing $V^{IV}OSO_4$ and of **1** are shown in Figure 10. The figure shows that complex **1** is a more potent inhibitor of FFA release when compared to $V^{IV}OSO_4$, but at higher concentrations the difference gradually decreases. Similarly, Figure 11 shows the concentration dependence of glucose uptake for $V^{IV}OSO_4$ and **1**. In the lower range of concentrations, the one closer to biologically relevant conditions, the complex is clearly more efficient than $V^{IV}OSO_4$.

The biological tests were carried out using water as solvent. It was concluded from the above that $[V^{IV}O(H_2pydmedpt)]^{2+}$ has pK_a values of about 6.9 and 7.9, the deprotonation sites being the pyridine nitrogens of the pyridoxal moiety. At pH 7.4, the predominant form of the complex is therefore $[V^{IV}O(Hpydmedpt)]^+$, but significant amounts of $[V^{IV}O(H_2pydmedpt)]^{2+}$ and $[V^{IV}O(pydmedpt)]$ are also present. All the species in solution may further significantly hydrolyze or, as revealed by the EPR and electronic spectra in aqueous solution, even partly oxidize to V^{V}-species. $V^{IV}OSO_4$ is present mainly in the form of $[(V^{IV}O)_2(OH)_5^-]_n$ at pH ∼7.4, it may oxidize extensively, and at higher concentrations $V^{IV}O(OH)_2$ may precipitate.[63] Moreover, both **1** and $V^{IV}O^{2+}$ may bind to components of the KRB buffer, namely, to BSA.[65] Therefore, it is plausible that the reason why **1**, and other insulin enhancing complexes previously studied, gives better EC_{50} and IC_{50} than $V^{IV}OSO_4$ in tests with cells, is mainly associated to the nature of the dominant vanadium species present in solution, which differ from those initially dissolved. In the present study it is $[V^{IV}O(Hpydmedpt)]^+$ in the case of **1** and $[(V^{IV}O)_2(OH)_5^-]_n$[63] in the case of $V^{IV}OSO_4$, their binding to BSA possibly being also relevant. The species found to be formed in methanol or DMSO may also be relevant here. Once vanadium enters the cells it can bind the target molecules for insulin enhancing activity of vanadium such as PTPase, PI3−K, GLUT, PKB, and PDE. Whatever may be the nature of the vanadium containing species responsible for the biological effect observed, these experiments clearly show that the EC_{50} and IC_{50} values of complex **1** are lower than for $V^{IV}OSO_4$, thereby indicating that **1** is an insulin enhancing agent, at least comparable to other complexes reported in the literature (Table 12)

CONCLUSIONS

A new Schiff base ligand $[H_4pydmedpt]^{2+}\cdot 2Cl^-$ derived from pyridoxal and medpt was obtained and characterized by analytical and spectroscopic methods. Its molecular structure was optimized by DFT procedures and some properties evaluated, namely, the donor properties of its potential donor atoms were estimated by the calculation of the Fukui function.

The preparation and characterization of the corresponding $V^{IV}O$-complex **1**, formulated as $[V^{IV}O(H_2pydmedpt)]^{2+}\cdot 2Cl^-$, protonated at both $N_{pyridine}$ atoms, is described. The molecular structure of the nonprotonated version, $[V^{IV}O(pydmedpt)]\cdot 5H_2O$,

was determined by single-crystal X-ray diffraction. The design of the ligand forced the binding of a phenolato group trans to the oxido group, a rare arrangement of the donor set for oxidovanadium complexes. This particular arrangement of donors decreases the distortion effect of the oxido group on the octrahedral geometry to the level not recorded so far, namely, the vanadium atom is displaced by only 0.17 Å from the equatorial leastsquares plane.

Spectroscopic studies, namely, EPR, confirmed the nature of the major species present in solution as similar to the one isolated in the solid state. Minor species were also detected in which one or two donor atoms are dissociated from the coordination sphere as originally present in the solid state. It was also found that the measured $|A_z|$ value for the major species present is lower than predicted from the additivity rule, this probably being because of the strong $V-O_{phenolate}$ bond trans to the O_{oxido} donor. Calculation of the EPR parameters by the DFT procedure as indicated by Garribba and co-workers[62] yielded a hyperfine coupling constant A_z in agreement with the experimental values, and confirming the influence of the $V-O_{phenolate}$ bond trans to the O_{oxido} donor on the $|A_z|$ value, decreasing it by about $6-7 \times 10^{-4}$ cm^{-1}. A few geometric characteristics and properties, such as $\pi-\pi$ stacking interactions between the pyridine rings, the basic character of the two $N_{pyridine}$ atoms, and UV−vis transitions could also be predicted by theoretical methods. These explain the spectroscopic results and support properties such as the two distinct pK_a values observed for $[V^{IV}O(H_2pydmedpt)]^{2+}$ in aqueous solution.

Experiments of % glucose uptake and inhibitory effects on FFA release with isolated rat adipocyte cells clearly showed that the EC_{50} and IC_{50} values of $[V^{IV}O(H_2pydmedpt)]^{2+}\cdot 2Cl^-$ are lower than for $V^{IV}OSO_4$, and of the same order of magnitude of several other established insulin enhancing complexes. Hence, the complex reported in this study is considered to be a potent insulin enhancing agent. In aqueous solution the species that predominates at pH 7.4 is $[V^{IV}O(Hpydmedpt)]^+$, but it is possible that BSA-$V^{IV}O$(pydmedpt) adducts are relevant for the insulin enhancing properties observed in the experiments with the adipocyte cells.

■ ASSOCIATED CONTENT

Supporting Information. Further details are given in Figures S1−S6 and Tables S1−S4. This material is available free of charge via the Internet at http://pubs.acs.org. The CCDC reference number for the cif file of **2** is 715 905.

■ AUTHOR INFORMATION

Corresponding Author
*E-mail: ars@klyuniv.ac.in.

■ ACKNOWLEDGMENT

The authors wish to record grateful thanks to Prof. P. K. Bharadwaj and Dr. Ramesh Thapliyal, Department of Chemistry, Indian Institute of Technology, Kanpur, for providing the single crystal structure, Prof. D. K. Mukherjee and Sourav Kundu, Department of Zoology, University of Kalyani, for providing laboratory facilities and fruitful discussions for the biological work, DST-FIST and UGC-SAP Programme for providing routine instrumental facilities, University of Kalyani for providing a fellowship (T.M.). J.C.P. and A.K. thank FEDER, Fundação para a Ciência e Tecnologia (FCT), SFRH/BPD/34835/2007 and PTDC/QUI-QUI/117477/2010 for financial support.

■ REFERENCES

(1) (a) Crans, D. C.; Smee, J. J.; Gaidamauskas, E.; Yang, L. *Chem. Rev.* **2004**, *104*, 849–902.(b) Rehder, D. *Bioinorganic Vanadium Chemistry*; John Wiley & Sons: New York, U.S.A., 2008; p 1−213.

(2) (a) Thompson, K. H.; Orvig, C. *Coord. Chem. Rev.* **2001**, *219−221*, 1033–1053. (b) Shechter, Y.; Goldwaser, I.; Mironchik, M.; Fridkin, M.; Gefel, D. *Coord. Chem. Rev.* **2003**, *237*, 3–11. (c) Thompson, K. H.; Orvig, C. *J. Inorg. Biochem.* **2006**, *100*, 1925–1935.

(3) Saltiel, A. R.; Kahn, C. R. *Nature* **2001**, *414*, 799–806.

(4) (a) Thompson, K. H.; McNeill, J. H.; Orvig, C. *Chem. Rev.* **1999**, *99*, 2561–2572. (b) Crans, D. C. *Vanadium Compounds: Chemistry, Biochemistry, and Therapeutic Applications*; Tracey, A. S., Ed.; American Chemical Society: Washington, DC, U.S.A., 1998; pp 259−269, 278−296, 308−368. (c) Li, M.; Smee, J. J.; Ding, W.; Crans, D. C. *J. Inorg. Biochem.* **2009**, *103*, 585–589. (d) Xie, M.; Li, L.; Yang, X.; Liu, W.; Yan, S.; Niu, Y.; Meng, Z. *Eur. J. Med. Chem.* **2010**, *45*, 2327–2335.

(5) (a) Orvig, C.; Thompson, K. H.; Liboiron, B. D.; McNeill J. H. Yuen, V. G. *J. Inorg. Biochem.* **2003**, *96*, 14–14. (b) Thompson, K. H.; Orvig, C. *Dalton Trans.* **2006**, 761–764.

(6) Thompson, K. H.; Lichter, J.; LeBel, C.; Scaife, M. C.; McNeill, J. H.; Orvig, C. *J. Inorg. Biochem.* **2009**, *103*, 554–558.

(7) Kawabe, K.; Yoshikawa, Y.; Adachi, Y.; Sakurai, H. *Life Sci.* **2006**, *78*, 2860–2866.

(8) (a) Sekar, N.; Li, J.; Shechter, Y. *Crit. Rev. Biochem. Mol. Biol.* **1996**, *31*, 339–359. (b) Fantus, I. G.; Tsiani, E. *Mol. Cell. Biochem.* **1998**, *182*, 109–119. (c) Molero, J. C.; Martinez, C.; Andres, A.; Satrustegui, J.; Carrascosa, J. M. *FEBS Lett.* **1998**, *425*, 298–304. (d) Mohammad, A.; Sharma, V.; McNeill, J. H. *Mol. Cell. Biochem.* **2002**, *233*, 139–143. (e) Scior, T.; Mack, H. G.; García, J. A.; Koch, W. *Drug Des. Dev. Ther.* **2009**, *2*, 221–231.

(9) (a) Evangelou, A. M. *Crit. Rev. Oncol. Hematol.* **2002**, *42*, 249–265. (b) Kostova, I. *Anti-Cancer Agents Med. Chem.* **2009**, *8*, 827–842. (c) Noblía, P.; Vieites, M.; Parajón-Costa, B. S.; Baran, E. J.; Cerecetto, H.; Draper., P.; González, M.; Piro, O. E.; Castellano, E. E.; Azqueta, A.; López de Ceráin, A.; Monge-Vega, A.; Gambino, D. *J. Inorg. Biochem.* **2005**, *99*, 443–451. (d) Abdelhamid, G.; Anwar-Mohamed, A.; Badary, O.; Moustafa, A.; El-Kadi, A. *Cell. Biol. Toxicol.* **2010**, *26*, 421–434. (e) D'Cruz, O. J.; Uckun, F. M. *Expert Opin. Invest. Drugs* **2002**, *11*, 1829–1836. (f) Papaioannou, A.; Manos, M.; Karkabounas, S.; Liasko, R.; Evangelou, A. M.; Correia, I.; Kalfakakou, V.; Costa Pessoa, J.; Kabanos, T. A. *J. Inorg. Biochem.* **2004**, *98*, 959–968.(g) Chatterjee, M.; Bishaye, A. . In *Vanadium in the Environment*; Nriagu, J. O., Ed.; John Wiley & Sons: New York, U.S.A., 1998; Vol. 31, pp 347−390.

(10) (a) Mishra, A. P.; Soni, M. *Met. Based Drugs* **2008**, *2008*, 875410. (b) Muhammad, N.; Ali, S.; Shahzadi, S.; Khan, A. *Russ. J. Coord. Chem.* **2008**, *34*, 448–453.

(11) Dong, Y.; Narla, R. K.; Sudbeck, E.; Uckun, F. M. *J. Inorg. Biochem.* **2000**, *78*, 321–330.

(12) Cohen, P. P. *Biochem. J.* **1939**, *33*, 1478–1487.

(13) Yanofsky, C.; Reissig, J. L. *J. Biol. Chem.* **1953**, *202*, 567–577.

(14) (a) Prior, F. G. R. *Med. Hypotheses* **1985**, *16*, 421–428. (b) Eto, I.; Krumdieck, C. L. *Adv. Exp. Med. Biol.* **1986**, *206*, 313–330.(c) Herbert, V. *Nutritional Factors in the Induction and Maintenance of Malignancy*; Butterworth, C. E., Hutchinson, M. L., Eds.; Academic Press: New York, U.S.A., 1983; pp 273−287. (d) Herbert, V. *Adv. Exp. Med. Biol.* **1986**, *206*, 293–311.(e) Bender, D. A. *Nutritional Biochemistry of the Vitamins*; Bender, D. A., Ed.; Cambridge University Press: New York, U.S.A., 1992; pp 223−268. (f) Bender, D. A.; Bowden, J. F.; Coulsen, W. F.; Dewji, M. R.; Sutton, J.; Symes, E. K. *Current Topics in Nutrition and Disease: Clinical and Physiological Applications of Vitamin B6*; Leklem, J. E., Reynolds, R. D., Ed.; Alan R. Liss: New York, U.S.A., 1988; pp 45−49.

(15) Richardson, D. R.; Tran, E.; Ponka, P. *Blood* **1995**, *86*, 4295–4306.

(16) (a) Metzler, D. E.; Longenecker, J. B.; Snell, E. E. *J. Am. Chem. Soc.* **1953**, *75*, 2786–2787. (b) Metzler, D. E.; Olivard, J.; Snell, E. E. *J. Am. Chem. Soc.* **1954**, *76*, 644–648.

(17) (a) Abbott, E. H.; Martell, A. E. *J. Am. Chem. Soc.* **1970**, *92*, 5845–5851. (b) Martell, A. E.; Eidson, A. F. *Bioinorg. Chem.* **1975**, *4*, 277–289. (c) Capasso, S.; Giordano, F.; Mattia, C.; Mazzarella, L.; Ripamonti, A. *J. Chem. Soc., Dalton Trans.* **1974**, 2228–2233. (d) Costa Pessoa, J.; Cavaco, I.; Correia, I.; Duarte, M. T.; Gillard, R. D.; Henriques, R. T.; Higes, F. J.; Madeira, C.; Tomaz, I. *Inorg. Chim. Acta* **1999**, *293*, 1–11.

(18) (a) Correia, I.; Costa Pessoa, J.; Duarte, M. T.; Henriques, R. T.; Piedade, M. F. M.; Veiros, L. F.; Jakusch, T.; Kiss, T.; Dörnyei, A.; Castro, M. M. C. A.; Geraldes, C. F. G. C.; Avecilla, F. *Chem.—Eur. J.* **2004**, *10*, 2301–2317. (b) Sundaravel, K.; Suresh, E.; Palaniandavar, M. *Inorg. Chim. Acta* **2009**, *362*, 199–207. (c) Correia, I.; Dornyei, A.; Avecilla, F.; Kiss, T.; Costa Pessoa, J. *Eur. J. Inorg. Chem.* **2006**, 656–662. (d) Correia, I.; Dornyei, A.; Jakusch, T.; Avecilla, F.; Kiss, T.; Costa Pessoa, J. *Eur. J. Inorg. Chem.* **2006**, 2819–2830. (e) Adão, P.; Maurya, M. R.; Kumar, U.; Avecilla, F.; Henriques, R. T.; Kusnetsov, M. L.; Costa Pessoa, J.; Correia, I. *Pure Appl. Chem.* **2009**, *81*, 1279–1296.

(19) (a) Hamana, K.; Niitsu, M.; Samejima, K. *Can. J. Bot.* **1998**, *76*, 130–133. (b) Hamana, K.; Matsuzaki, S. *J. Biochem.* **1982**, *91*, 1321–1328.

(20) (a) Prakash, N. J.; Bowlin, T. L.; Davis, G. F.; Sunkara, P. S.; Sjoerdsma, A. *Anticancer Res.* **1988**, *8*, 563–568. (b) Sunkara, P. S.; Zwolshen, J. H.; Prakash, N. J.; Bowlin, T. L. *Adv. Exp. Med. Biol.* **1988**, *250*, 707–716.

(21) Kawabe, K.; Suekuni, T.; Inada, T.; Yamato, K.; Tadokoro, M.; Kojima, Y.; Fujisawa, Y.; Sakurai, H. *Chem. Lett.* **1998**, *27*, 1155–1156.

(22) (a) Sakurai, H.; Yoshikawa, Y.; Yasui, H. *Chem. Soc. Rev.* **2008**, *37*, 2383–2392. (b) Sakurai, H.; Kojima, Y.; Yoshikawa, Y.; Kawabe, K.; Yasui, H. *Coord. Chem. Rev.* **2002**, *226*, 187–198. (c) Crans, D. C. *J. Inorg. Biochem.* **2000**, *80*, 123–131. (d) Sakurai, H.; Yoshikawa, Y.; Yasui, H. *Chem. Soc. Rev.* **2008**, *37*, 2383–2392.

(23) Vogel, A. I. *A text-book of quantitative inorganic analysis, including elementary instrumental analysis*; Longman: London, U.K., 1962; pp 808−809, 790−791.

(24) Rockenbauer, A.; Korecz, L. *Appl. Magn. Reson.* **1996**, *10*, 29–43.

(25) *SAINT-Plus*, Version 6.45; Bruker AXS Inc.: Madison, WI, 2003.

(26) Sheldrick, G. M. *SADABS*; Bruker AXS Inc.: Madison, WI, 1997.

(27) Altomare, A.; Cascarano, G.; Giacovazzo, C.; Guagliardi, A.; Burla, M. C.; Polidori, G.; Camalli, M. *J. Appl. Crystallogr.* **1994**, *27*, 435.

(28) Sheldrick, G. M. *SHELXTL NT*, Version 5.1, Program for Solution and Refinement of Crystal Structures; University of Göttingen: Göttingen, Germany, 1997.

(29) Farrugia, L. J. *J. Appl. Crystallogr.* **1999**, *32*, 837–838.

(30) Frisch, M. J.; Trucks,G. W.; Schlegel, H. B.; Scuseria, G. E.; Robb, M. A.; Cheeseman, J. R.; Montgomery, J. A.; Vreven, Jr., T.; Kudin, K. N.; Burant, J. C.; Millam, J. M.; Iyengar, S. S.; Tomasi, J.; Barone, V.; Mennucci, B.; Cossi, M.; Scalmani, G.; Rega, N.; Petersson, G. A.; Nakatsuji, H.; Hada, M.; Ehara, M.; Toyota, K.; Fukuda, R.; Hasegawa, J.; Ishida, M.; Nakajima, T.; Honda, Y.; Kitao, O.; Nakai, H.; Klene, M.; Li, X.; Knox, J. E.; Hratchian, H. P.; Cross, J. B.; Adamo, C.; Jaramillo, J.; Gomperts, R.; Stratmann, R. E.; Yazyev, O.; Austin, A. J.; Cammi, R.; Pomelli, C.; Ochterski, J. W.; Ayala, P. Y.; Morokuma, K.; Voth, G. A.; Salvador, P.; Dannenberg, J. J.; Zakrzewski, V. G.; Dapprich, S.; Daniels, A. D.; Strain, M. C.; Farkas, O.; Malick, D. K.; Rabuck, A. D.; Raghavachari, K.; Foresman, J. B.; Ortiz, J. V.; Cui, Q.; Baboul, A. G.; Clifford, S.; Cioslowski, J.; Stefanov, B. B.; Liu,G.; Liashenko, A.; Piskorz, P.; Komaromi, I.; Martin, R. L.; Fox, D. J.; Keith, T.; Al-Laham, M. A.; Peng, C. Y.; Nanayakkara, A.; Challacombe, M.; Gill, P. M. W.; Johnson, B.; Chen, W.; Wong, M. W.; Gonzalez, C.; Pople, J. A. *Gaussian 03*, Revision A.1; Gaussian, Inc.: Pittsburgh, PA, 2003.

(31) (a) Becke, A. D. *Phys. Rev. A* **1988**, *38*, 3098–3100. (b) Lee, C.; Yang, W.; Parr, R. G. *Phys. Rev. B* **1988**, *37*, 785–789.

(32) Ditchfield, R.; Hehre, W. J.; Pople, J. A. *J. Chem. Phys.* **1971**, *54*, 724–728.

(33) Liu, T.; Gu, J.; Tan, X. J.; Zhu, W. L.; Luo, X. M.; Jiang, H. L.; Ji, R. Y.; Chen, K. X.; Silman, I.; Sussman, J. L. *J. Phys. Chem. A* **2001**, *105*, 5431–5437.

(34) Yang, W.; Mortier, W. J. *J. Am. Chem. Soc.* **1986**, *108*, 5708–5711.

(35) Adamo, C.; Barone, V. *J. Chem. Phys.* **1998**, *108*, 664–675.

(36) (a) Burke, K.; Perdew, J. P.; Wang, Y. *Electronic Density Functional Theory: Recent Progress and New Directions*; Dobson, J. F., Vignale, G., Das, M. P., Eds.; Plenum Press: New York, U.S.A., 1998. (b) Perdew, J. P. *Electronic Structure of Solids '91*; Ziesche, P., Eschrig, H., Eds.; Akademie Verlag: Berlin, Germany, 1991. p 11. (c) Perdew, J. P.; Chevary, J. A.; Vosko, S. H.; Jackson, K. A.; Pederson, M. R.; Singh, D. J.; Fiolhais, C. *Phys. Rev. B* **1992**, *46*, 6671–6687. (d) Perdew, J. P.; Chevary, J. A.; Vosko, S. H.; Jackson, K. A.; Pederson, M. R.; Singh, D. J.; Fiolhais, C. *Phys. Rev. B* **1993**, *48*, 11638–11645. (e) Perdew, J. P.; Burke, K.; Wang, Y. *Phys. Rev. B* **1996**, *54*, 16533–16539.

(37) (a) Lee, C.; Yang, W.; Parr, R. G. *Phys. Rev. B* **1988**, *37*, 785–789. (b) Becke, A. D. *J. Chem. Phys.* **1992**, *97*, 9173–9177. (c) Perdew, J. P. *Phys. Rev. B* **1986**, *33*, 8822–8824.

(38) (a) Wachters, A. J. H. *J. Chem. Phys.* **1970**, *52*, 1033–1034. (b) Hay, P. J. *J. Chem. Phys.* **1977**, *66*, 4377–4384. (c) McLean, A. D.; Chandler, G. S. *J. Chem. Phys.* **1980**, *72*, 5639–5648. (d) Krishnan, R.; Binkley, J. S.; Seeger, R.; Pople, J. A. *J. Chem. Phys.* **1980**, *72*, 650–654. (e) Raghavachari, K.; Trucks, G. W. *J. Chem. Phys.* **1989**, *91*, 1062–1065.

(39) Skripnikov, L. *Chemissian*, version 2.000; 2005−2010; http://www.chemissian.com.

(40) Adachi, Y.; Sakurai, H. *Chem. Pharm. Bull.* **2004**, *52*, 428–443.

(41) Itaya, K.; Ui, M. *J. Lipid Res.* **1965**, *6*, 16–20.

(42) (a) Yang, W. T.; Mortier, W. J. *J. Am. Chem. Soc.* **1986**, *108*, 5708–5711. (b) Kostova, I.; Trendafilova, N.; Mihaylov, T. *Chem. Phys.* **2005**, *314*, 73–84. (c) Kostova, I.; Trendafilova, N.; Momekov, G. *J. Inorg. Biochem.* **2005**, *99*, 477–487.

(43) Macrae, C. F.; Edgington, P. R.; McCabe, P.; Pidcock, E.; Shields, G. P.; Taylor, R.; Towler, M.; Van de Streek, J. *J. Appl. Crystallogr.* **2006**, *39*, 453–457.

(44) (a) Yuan, C.; Lu, L.; Gao, X.; Wu, Y.; Guo, M.; Li, Y.; Fu, X.; Zhu, M. *J. Biol. Inorg. Chem.* **2009**, *14*, 841–851. (b) Maurya, M. R.; Kumar, A.; Ebel, M.; Rehder, D. *Inorg. Chem.* **2006**, *45*, 5924–5937. (c) Amin, S. S.; Cryer, K.; Zhang, B.; Dutta, S. K.; Eaton, S. S.; Anderson, O. P.; Miller, S. M.; Reul, B. A.; Brichard, S. M.; Crans, D. C. *Inorg. Chem.* **2000**, *39*, 406–416.(d) Boas, L. V.; Costa Pessoa, J. *Comprehensive Coordination Chemistry*; Wilkinson, G., Gillard, R. D., McCleverty, J. A., Eds.; Oxford: Oxford, U.K., 1987; Vol. 3, pp 453−583 and refs therein. (e) Crans, D. C.; Smee, J. J. *Comprehensive Coordination Chemistry II*; McCleverty, J. A., Meyer, T. J., Eds.; Elsevier: Amsterdam, The Netherlands, 2004; Vol. 4, pp 176−239.

(45) Cornman, C. R.; Kampf, J.; Lah, M. S.; Pecoraro, V. L. *Inorg. Chem.* **1992**, *31*, 2035–2043.

(46) Gätjens, J.; Meier, B.; Kiss, T.; Nagy, E. M.; Buglyó, P.; Sakurai, H.; Kawabe, K.; Rehder, D. *Chem.—Eur. J.* **2003**, *9*, 4924–4935.

(47) Smith, T. S.; Root, C. A.; Kampf, J. W.; Rasmussen, P. G.; Pecoraro, V. L. *J. Am. Chem. Soc.* **2000**, *122*, 767–775.

(48) Seifert, H. J.; Uebach, J. *Z. Anorg. Allg. Chem.* **1981**, *479*, 32–40.

(49) Baruah, B.; Das, S.; Chakravorty, A. *Inorg. Chem.* **2002**, *41*, 4502–4508.

(50) Turel, I.; Golobič, A.; Klavžar, A.; Pihlar, B.; Buglyó, P.; Tolis, E.; Rehder, D.; Sepčić, K. *J. Inorg. Biochem.* **2003**, *95*, 199–207.

(51) Sokolowski, A.; Adam, B.; Weyhermüller, T.; Kikuchi, A.; Hildenbrand, K.; Schnepf, R.; Hildebrandt, P.; Bill, E.; Wieghardt, K. *Inorg. Chem.* **1997**, *36*, 3702–3710.

(52) (a) Mohan, M.; Holmes, S. M.; Butcher, R. J.; Jasinski, J. P.; Carrano, C. J. *Inor Chem.* **1992**, *31*, 2029–2034. (b) Zhang, Y.; Holm, R. H. *Inorg. Chem.* **1990**, *29*, 911–917.

(53) Crans, D. C. *Pure Appl. Chem.* **2005**, *77*, 1497–1527.

(54) Noguera, M.; Ríos-Font, R.; Rodríguez-Santiago, L.; Solans-Monfort, X.; Oliva, A.; Bertran, J.; Sodupe, M. *Theor. Chem. Acc.* **2009**, *123*, 105–111.

(55) Kawabe, K.; Tadokoro, M.; Ichimura, A.; Kojima, Y.; Takino, T.; Sakurai, H. *J. Am. Chem. Soc.* **1999**, *121*, 7937–7938.
(56) Wüthrich, K. *Helv. Chim. Acta* **1965**, *48*, 1012–1017.
(57) Chasteen, N. D. *Biological Magnetic Resonance*; Reuben, J., Ed.; Plenum: New York, U.S.A., 1981; p 53.
(58) Costa Pessoa, J.; Calhorda, M. J.; Cavaco, I.; Costa, P. J.; Correia, I.; Costa, D.; Vilas-Boas, L. F.; Félix, V.; Gillard, R. D.; Henriques, R. T.; Wiggins, R. *Dalton Trans.* **2004**, 2855–2866.
(59) Rehder, D. *Bioinorganic Vanadium Chemistry*; John Wiley & Sons: New York, U.S.A., 2008; pp 67−74.
(60) (a) Munzarová, M. T. L.; Kaupp, M. *J. Phys. Chem. B* **2001**, *105*, 12644–12652. (b) Saladino, A. C.; Larsen, S. C. *J. Phys. Chem. A* **2003**, *107*, 1872–1878. (c) Neese, F. *J. Chem. Phys.* **2003**, *118*, 3939–3948. (d) Costa Pessoa, J.; Calhorda, M. J.; Cavaco, I.; Correia, I.; Duarte, M. T.; Felix, V.; Henriques, R. T.; Piedade, M. F. M.; Tomaz, T. *J. Chem. Soc., Dalton Trans.* **2002**, 4407–4415.
(61) Micera, G.; Garribba, E. *Dalton Trans.* **2009**, 1914–1918.
(62) (a) Gorelsky, S.; Micera, G.; Garribba, E. *Chem.—Eur. J.* **2010**, *16*, 8167–8180. (b) Lodyga-Chruscinska, E.; Micera, G.; Garribba, E. *Inorg. Chem.* **2011**, *50*, 883–899.
(63) Costa Pessoa, J.; Boas, L. V.; Gillard, R. D.; Lancashire, R. J. *Polyhedron* **1988**, *7*, 1245–1262.
(64) *BioDataFit*, version 1.02, Data Fit for Biologists; Chang Bioscience Inc.: Castro Valley, CA, 2008; (http//www.chang-bioscience.com/stat/ec50.html).
(65) Costa Pessoa, J.; Tomaz, I. *Curr. Med. Chem.* **2010**, *17*, 3701–3738.
(66) Sakurai, H.; Watanabe, H.; Tamura, H.; Yasui, H.; Matsushita, R.; Takada, J. *Inorg. Chim. Acta* **1998**, *283*, 175–183.
(67) Karmaker, S.; Saha, T. K.; Yoshikawa, Y.; Yasui, H.; Sakurai, H. *J. Inorg. Biochem.* **2006**, *100*, 1535–1546.
(68) Kawabe, K.; Sasagawa, T.; Yoshikawa, Y.; Ichimura, A.; Kumekawa, K.; Yanagihara, N.; Takino, T.; Sakurai, H.; Kojima, Y. *J. Biol. Inorg. Chem.* **2003**, *8*, 893–906.
(69) Nakai, M.; Obata, M.; Sekiguchi, F.; Kato, M.; Shiro, M.; Ichimura, A.; Kinoshita, I.; Mikuriya, M.; Inohara, T.; Kawabe, K.; Sakurai, H.; Orvig, C.; Yano, S. *J. Inorg. Biochem.* **2004**, *98*, 105–112.